

PACS numbers: 68.37.Hk, 81.16.Hc, 82.30.Vy, 83.80.Mc

## **Optimization of Biodiesel Production from Refined Oil Blend Using a Heterogeneous Nanoparticle Catalyst**

Heba Naseef, Reem Tulaimat, Seba Naseef, and Jasim Alebrahim

*Department of Chemistry, Faculty of Sciences,  
Homs University,  
Homs, Syria*

This study focuses on optimizing biodiesel production from a refined blend of palm and cottonseed oils, utilizing the MCM-41 nanocatalyst. Palm oil biodiesel is noted for its excellent oxidative stability, but demonstrates poor low-temperature flow properties due to its high-saturated fatty acid content. In contrast, cottonseed oil biodiesel offers enhanced flow properties at low temperatures, but exhibits lower oxidative stability. By blending these two oils, this study aims to maximize biodiesel yield and achieve improved overall fuel properties. The esterification process is optimized using a traditional experimental approach, varying two parameters simultaneously, while maintaining the others constant. The critical variables studied include the molar ratio of alcohol-to-oil, catalyst amount, reaction temperature, and reaction time. The MCM-41 nanocatalyst, a mesoporous silica material with nanoscale features, is selected due to its high surface area, uniform pore distribution, and superior catalytic performance. This methodical approach simplifies the optimization process, reduces experimental complexity, and provides a practical framework for identifying optimal reaction conditions in resource-limited environments.

Це дослідження зосереджено на оптимізації виробництва біодизеля з очищеної суміші пальмової та бавовняної олій з використанням нанокаталізатора МСМ-41. Біодизель з пальмової олії відомий своєю чудовою окиснювальною стабільністю, але демонструє погані низькотемпературні властивості плинності через високий вміст насичених жирних кислот. Навпаки, біодизель з бавовняної олії пропонує поліпшені властивості плинності за низьких температур, але демонструє нижчу окиснювальну стабільність. Змішуючи ці дві олії, дослідження має на меті максимізувати вихід біодизеля та досягти поліпшених загальних властивостей палива. Процес етерифікації був оптимізований за допомогою традиційного експериментального підходу з одночасним змінюванням двох параметрів, а інші залишалися постійними. Досліджувані критичні змінні включали молярне співвідношення спирту до олії, кількість

каталізатора, температуру реакції та час реакції. Нанокаталізатор MCM-41, тобто мезопористий кремнеземний матеріал з нанорозмірними характеристиками, був обраний завдяки своїй великій площі поверхні, рівномірному розподілу пор і чудовій каталітичній продуктивності. Цей методичний підхід спрощує процес оптимізації, зменшує експериментальну складність і забезпечує практичну основу для визначення оптимальних умов реакції в умовах обмежених ресурсів.

**Key words:** optimization, esterification, transesterification, MCM-41, biodiesel.

**Ключові слова:** оптимізація, етерифікація, переетерифікація, MCM-41, біодизель.

*(Received 29 November, 2024)*

## 1. INTRODUCTION

The global energy demand is met through a diverse mix of energy sources. Statistics indicate that oil accounts for 35% of the global energy supply, followed by coal at 29% and natural gas at 24%. Hydropower contributes 6%, while nuclear energy provides 5%, and the remaining 1% comes from alternative energy sources. Despite the dominance of fossil fuels as the primary energy source, they are finite and non-renewable. At current consumption rates, the estimated reserves of oil, natural gas, and coal are expected to last approximately 45, 60, and 120 years, respectively [1].

The 21-st century has introduced significant challenges, including the urgent need for sustainable energy sources, increasing environmental degradation, and rising fossil fuel costs [2]. A notable surge in fuel consumption in recent years [3] has amplified global warming, largely due to the emission of pollutants [4]. This environmental pollution has profound health effects, with air pollution accounting for around 4.2 million deaths each year from chronic illnesses such as cardiovascular disease, strokes, and lung cancer. Furthermore, it is troubling that almost 91% of the world's population lives in areas, where air quality does not match the World Health Organization's criteria [5]. To reduce reliance on petroleum, mitigate its impact on climate change, and lower economic burdens, biofuels have emerged as a promising alternative in the transportation sector [6].

Biofuels are any fuel formed from organic materials, known as biomass, whether plant-based or animal-based, which can be burned to generate energy. They are considered as sustainable and environmentally friendly substitutes to fossil fuels like oil, coal, and natural gas [7]. Like fossil fuels, biofuels exist in different forms: gaseous biofuels such as methane derived from the decomposition of

organic matter, liquid biofuels like biodiesel extracted from vegetable oils, recycled wax, or animal fats, and bioethanol, an alcohol produced from fermenting sugars and starchy crops like corn [8]. Among these options, biodiesel stands out as the most viable choice, accounting for approximately 82% of total biofuel production [9]. Biodiesel plays a crucial role in addressing energy needs across various environments, from industrial zones to residential areas, urban centres to rural regions, and small to large-scale applications, all while achieving an impressive balance in net energy output [10].

Diesel is a liquid fuel composed of hydrocarbons, produced from petroleum through fractional distillation at temperatures ranging from 200 to 350°C. A single barrel (42 gallons) of crude oil can yield approximately 10 gallons of diesel. Diesel and gasoline are not interchangeable as fuels due to differences in engine requirements. Diesel boasts a higher energy content (38.3 MJ·L<sup>-1</sup>) compared to gasoline (34.7 MJ·L<sup>-1</sup>). It is a primary fuel for diesel engines and plays a significant role in heating homes, particularly in developed countries. Diesel engines power most heavy machinery and equipment, including tractors, trucks, construction machines, mining equipment, and military vehicles, reflecting differences in combustion mechanisms [1].

Biodiesel, on the other hand, is a yellow combustible liquid that closely resembles fossil diesel but is derived from renewable biological sources such as plant oils and animal fats [11]. Table 1 provides a comparison of the specifications for fossil diesel and biodiesel based on the standards set by the American Society for Testing and Materials (ASTM) [12, 13].

Biodiesel is a biodegradable fuel, which promotes natural breakdown and reduces harmful environmental effects [15]. Biodiesel also

**TABLE 1.** Comparison between fossil diesel and biodiesel according to ASTM standards.

| Property                        | Biodiesel      | Fossil Diesel         |
|---------------------------------|----------------|-----------------------|
| Composition                     | FAME (C12–C22) | Hydrocarbon (C10–C21) |
| Flash point, K                  | 373–443        | 333–353               |
| Specific gravity, g/mL          | 0.88           | 0.85                  |
| Cloud point, K                  | 270–285        | 258–278               |
| Pour point, K                   | 258–289        | 243–258               |
| Carbon content, wt. %           | 77             | 87                    |
| Cetane number                   | 48–60          | 40–55                 |
| Sulphur content, wt. %          | 0.05           | 0.05                  |
| Hydrogen content, wt. %         | 12             | 13                    |
| Kinematic viscosity (40°C), cSt | 4.0–6.0        | 1.3–4.1               |

exhibits lower toxicity, leading to decreased emissions of harmful compounds [16]. Unlike fossil diesel, biodiesel contains only trace amounts of aromatic and sulphur compounds and has an oxygen content ranging from 10% to 11% by weight. This oxygen presence allows for complete combustion, resulting in a significant reduction in emissions of hydrocarbons, carbon monoxide, and particulate matter [17]. Due to its renewable nature, biodiesel can provide a dependable energy supply. Additionally, the high flash point of biodiesel makes it non-flammable and less likely to ignite or explode, improving safety during storage and transportation compared to fossil diesel, which has a lower flash point [18–20]. Biodiesel also offers excellent lubricating properties, outperforming fossil diesel by up to 66%, thanks to the presence of methyl or ethyl esters, which act as natural lubricants. These compounds help reduce friction and wear between moving parts in the engine. As a result, biodiesel can decrease engine wear from extended use, leading to longer lifespans and reduced maintenance costs [14].

The scope of this study focusing on MCM-41, a mesoporous silica catalyst known for its high surface area and catalytic efficiency, was used to optimize the transesterification process. By adjusting two variables at a time while keeping the others constant, this research aims to identify the optimal conditions for biodiesel production, offering a cost-effective and practical method for producing high-quality biodiesel from refined oil blends. The results of this study contribute to advancing biodiesel production technology and support its adoption as a viable and sustainable alternative energy source.

## 2. EXPERIMENTAL

### 2.1. Materials

Sodium metasilicate ( $\text{Na}_2\text{SiO}_3 \cdot 5\text{H}_2\text{O}$ ), with 97% purity, sourced from BDH, was used as the silica precursor, while cetyltrimethylammonium bromide (CTAB) ( $\text{C}_{19}\text{H}_{42}\text{BrN}$ ), with 99% purity, also from BDH, served as the templating agent. Sulphuric acid ( $\text{H}_2\text{SO}_4$ ), with 97% purity from BDH, was employed as a pH-modifying additive, and deionized water was used as the solvent. For the biodiesel production, refined palm oil and refined cottonseed oil were utilized as feedstocks, and methanol ( $\text{CH}_3\text{OH}$ ), with 99% purity from BDH, was used as the alcohol in the esterification process.

### 2.2. Preparation of the Catalyst

The MCM-41 catalyst was prepared by first dissolving 2.5 grams of

sodium metasilicate ( $\text{Na}_2\text{SiO}_3 \cdot 5\text{H}_2\text{O}$ ) in diluted water and slowly adding it to a 10% cetyltrimethylammonium bromide (CTAB) solution in deionized water, while stirring vigorously for 2 hours. The pH was adjusted to 11 using a 1 N sulphuric acid solution, and mixing continued for another 2 hours. The mixture was transferred to a Teflon-lined stainless-steel autoclave, heated to  $120^\circ\text{C}$ , and maintained for 48 hours under hydrothermal pressure. After cooling, the precipitate was separated, washed with deionized water, and dried at  $80^\circ\text{C}$  for 24 hours. The organic template was then removed by calcination in a furnace, heating at  $2^\circ\text{C}$  per minute to  $550^\circ\text{C}$  and maintaining this temperature for 6 hours.

### 2.3. Preparation of the Refined Oil

Palm oil and cottonseed oil were mixed in a 50v/50v ratio. To obtain a homogeneous blend, the mixture was stirred using a magnetic stirrer for two hours, while being heated to  $100^\circ\text{C}$  to remove any water content, as shown in Fig. 1.

### 2.4. Esterification of Fatty Acids in the Oil Blend

The direct esterification reaction was carried out using a 250 mL round-bottom flask with two openings. One opening was connected to a reflux condenser to minimize the loss of evaporated methanol, while the other opening was left open for the addition of chemicals and withdrawal of samples. The flask, containing only the oil, was placed in a water bath, and the oil was heated to the required temperature. Once the desired temperature was reached, the methanol-catalyst was introduced into the system.



Fig. 1. Preparation method of the refined blend of cottonseed and palm oils.

Given the poor miscibility between methanol and oil, magnetic stirring was maintained at a constant speed of 600 rpm throughout the reaction to ensure optimal mixing [21]. At regular intervals, 2 mL aliquots were extracted until the reaction reached 120 minutes. Each sample was immediately washed with water to halt the reaction and facilitate phase separation. To enhance the separation process, the aliquots were allowed to settle for 30 minutes. A small sample was collected from the upper (oil) layer. For titration, the sample was diluted by adding it to a mixture of ethanol and ether. Phenolphthalein was used as the indicator. The acid value ( $A_v$ ) was determined by titrating the sample with a 0.02 N KOH solution, in accordance with standard procedures (AOCS Ca 5a-40). The volume of KOH required to produce a pink colour in the sample was recorded. Conversion efficiency was then calculated using the following equation:

$$X_F[\%] = \left( (A_{v_0} - A_v) / A_{v_0} \right) \cdot 100\% ;$$

here,  $A_{v_0}$  is the acid value at the initial time (before the reaction),  $A_v$  is the acid value at the reaction time  $t$ ,  $X_F$  is the conversion rate.

### 3. RESULTS AND DISCUSSION

#### 3.1. SEM Analysis for MCM-41

Scanning electron microscopy (SEM) uses a focused beam of high-energy electrons to scan a sample's surface, producing detailed images by analysing the interaction of the electrons with the atoms in the sample. The beam is scanned in a point-by-point pattern, with the intensity of the detected signal creating the image. As shown in Figure 2, the SEM image of the catalyst indicates that most particles are small, ranging from 30–50 nm, spherical, and highly homogeneous.

#### 3.3. XRD Analysis

Figure 3 shows the pattern XRD of the prepared and calcinated MCM-41 sample at 550°C for 6 hours, within the  $2\theta$  range of 1–10°, revealing a prominent and robust peak ( $d100$ ) at  $2\theta = 1.1^\circ$ .

Calculations were performed to determine the dimensions of the resulting crystals using Scherrer equation [22]:

$$D = \frac{K\lambda}{\beta_{FWHM} \cos(\theta)} ,$$

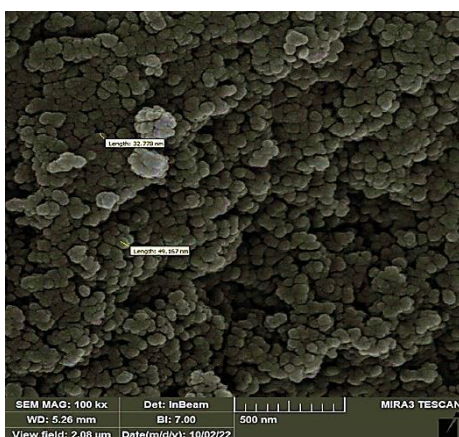


Fig. 2. The SEM image of the MCM-41 material with nanoscale dimensions.

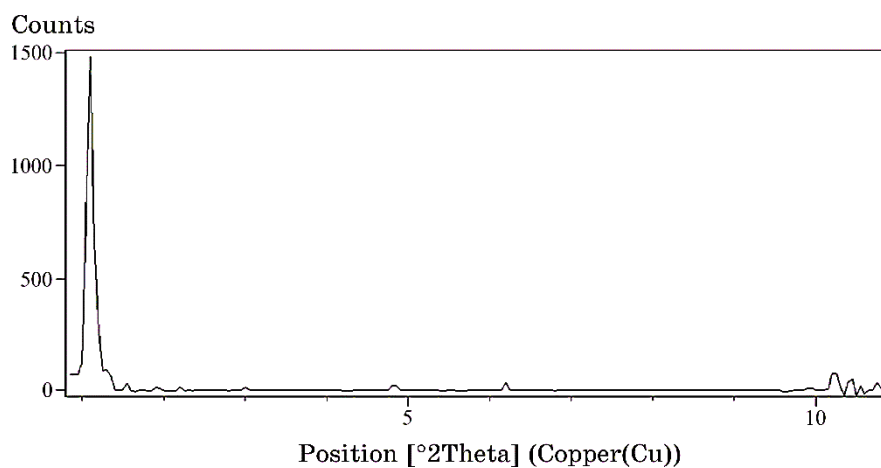


Fig. 3. X-ray diffraction pattern of calcinated MCM-41 catalyst.

where  $K$  is a constant with a value of (0.94);  $\lambda$  is x-ray wavelength used in XRD and its value is of 0.1540 nm for the copper element;  $\beta_{FWHM}$  is the peak width at half maximum is measured in radians, and  $D$  represents the crystal dimensions in nanometres;  $\theta$  is x-ray diffraction angle.

The calculated and measured values in Table 2 confirm the achievement of nanoscale dimensions. By examining the values  $D$ , we find that the prepared catalyst MCM-41 has nanoscale dimensions, with particle size in the order of 38.9397 nm. This is consistent with the results obtained from the scanning electron microscope. This will enhance its catalytic effectiveness in various chemi-

**TABLE 2.** Results of XRD data for MCM-41 catalyst.

| $2\theta$ | $\Theta$ , rad | FWHM   | $\beta_{FWHM}$ | $D$ , nm |
|-----------|----------------|--------|----------------|----------|
| 1.1       | 0.009599       | 0.2131 | 0.003719       | 38.9397  |

cal and industrial applications.

### 3.4. Effect of Various Factors on the Esterification of Free Fatty Acids

The effect of various factors on the direct acid esterification reaction was investigated, including the methanol-to-oil molar ratio ( $M$ ), catalyst amount ( $A$ ), reaction temperature ( $T$ ), and reaction time ( $D$ ). The study focused on analysing the influence of two factors simultaneously, while the values of the other two factors were kept constant at their optimal conversion conditions. This approach allowed a comprehensive understanding of how each variable affects the esterification process.

#### 3.4.1. Effect of Reaction Time ( $D$ ) and Temperature ( $T$ )

The effects of reaction time ( $D$ ) and temperature ( $T$ ) on the esterification of pure and used oil blends were investigated, with the molar ratio ( $M$ ) and catalyst amount ( $A$ ) maintained at their optimal values. The molar ratio ( $M$ ) was set at 1:6, and the catalyst amount was 0.05 g. As depicted in Fig. 4, increasing the temperature from 50°C to 60°C significantly enhanced conversion, particularly after 40 minutes of reaction time. Higher temperatures and extended reaction times promote conversion by improving the mixing of reactants and enhancing molecular mobility. However, it is important to ensure that the temperature does not approach methanol boiling point, as evaporation at higher temperatures can reduce conversion efficiency.

#### 3.4.2. Effect of the Methanol-to-Oil Ratio ( $M$ ) and Catalyst Amount ( $A$ )

The effects of the methanol-to-oil ratio ( $M$ ) and catalyst amount ( $A$ ) on esterification of refined oil blend was studied, keeping the temperature ( $T$ ) at 60°C and reaction time ( $D$ ) at 50 minutes, increasing the methanol-to-oil ratio 1:3, 1:4, 1:5, 1:6 with 0.05 g of catalyst-improved conversion, peaking at 40.5% at the 1:6 ratio. However, using 0.1 g of catalyst further increased conversion, and the methanol ratio continued to influence positively esterification. These re-

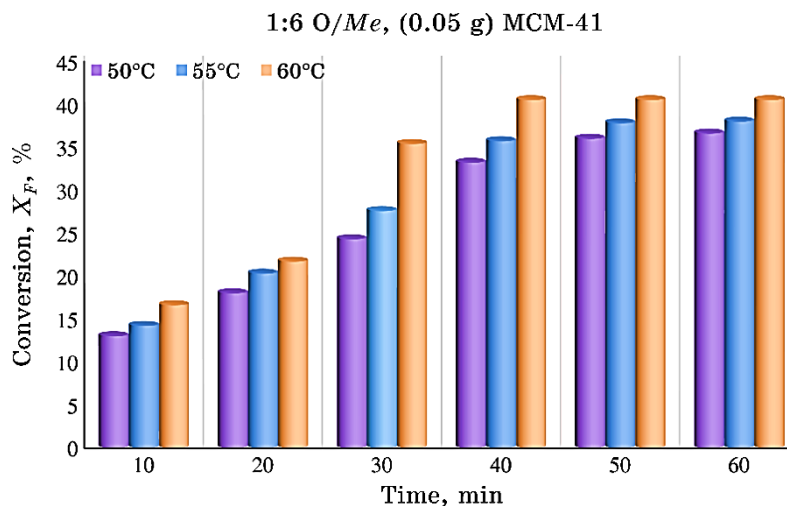


Fig. 4. Effect of reaction time and temperature on the conversion rate of the refined blend.

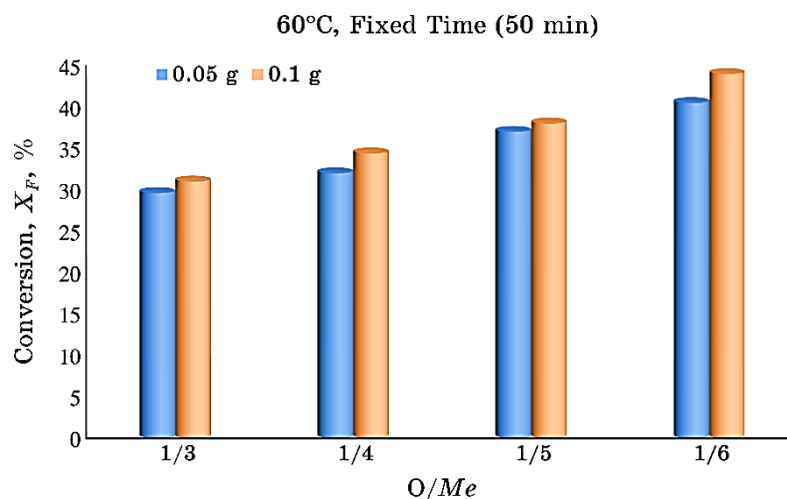


Fig. 5. Effect of methanol-to-oil ratio ( $M$ ) and catalyst amount ( $A$ ) on the conversion of the refined blend.

sults suggest that increasing both methanol and catalyst amounts enhances conversion as shown in Fig. 5.

### 3.4.3. Effect of the Methanol-to-Oil Ratio ( $M$ ) and Temperature ( $T$ )

Figure 6 illustrates that increasing the methanol-to-oil ratio ( $M$ )

from 1:3 to 1:6 improves the conversion rate, especially when combined with higher temperatures.

At a 1:3 ratio and 60°C, the esterification yield for blend reached 31%, which is considered adequate given the low free fatty acid content, as the methanol was sufficient to convert most of the acids into ester. Further increases in the methanol ratio to 1:4 resulted in a rise in conversion, reaching the highest conversion at a 1:6 ratio and 60°C.

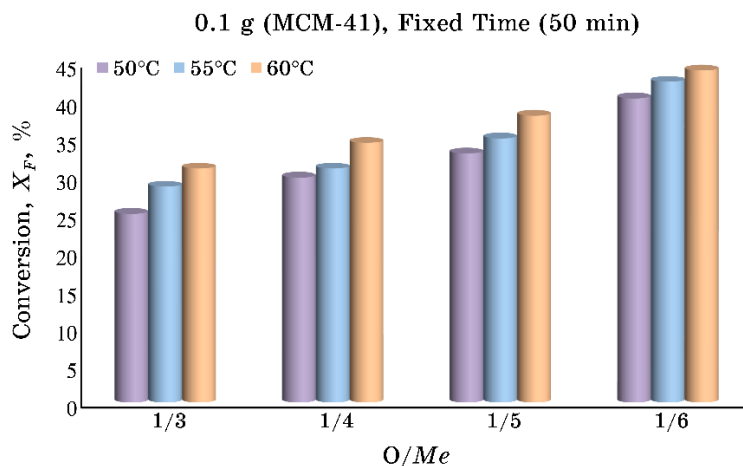


**Fig. 6.** Effect of methanol-to-oil ratio ( $M$ ) and temperature ( $T$ ) on the conversion of the refined blend.

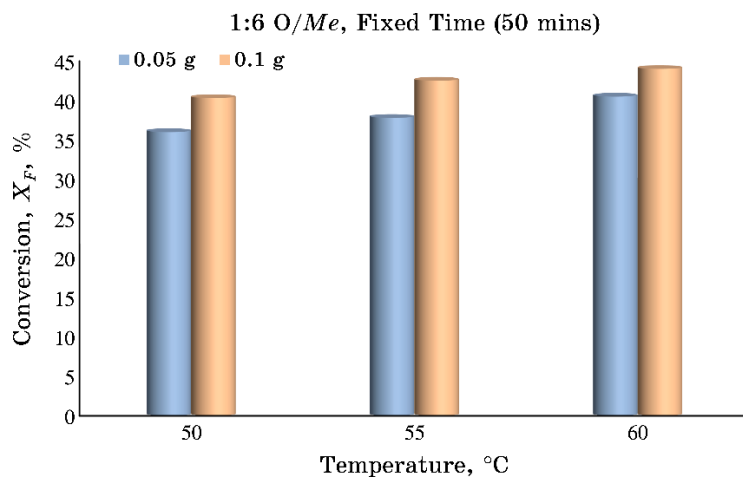


**Fig. 7.** Effect of catalyst amount ( $A$ ) and temperature ( $T$ ) on the conversion of the refined blend.

#### **3.4.4. Effect of Catalyst Amount ( $A$ ) and Temperature ( $T$ )**

The effect of catalyst amount ( $A$ ) and reaction temperature ( $T$ ) on the conversion of free fatty acids (FFAs) to esters was investigated at a constant reaction time of 50 minutes and a methanol-to-oil ratio ( $M$ ) of 1:6 for the blend. Figure 7 demonstrates that increasing the amount of MCM-41 catalyst from 0.05 g to 0.1 g enhances significantly the conversion, especially at higher temperatures. This improvement is due to the unique mesoporous structure of MCM-41, which provides a large surface area and numerous active sites, facilitating more effective interaction between the reactants. The high thermal stability of MCM-41 ensures efficient catalytic performance even at elevated temperatures, further boosting the conversion rate.

#### **3.4.5. Effect of Methanol-to-Oil Ratio ( $M$ ) and Reaction Time ( $D$ )**

The impact of the methanol-to-oil ratio ( $M$ ) and reaction time ( $D$ ) on the conversion of free fatty acids (FFA) to esters was evaluated, maintaining a reaction temperature of 60°C and catalyst concentrations of 0.1 g for the refined blend. As shown in Fig. 8, the pure blend exhibited a notable increase in FFA conversion over time, reaching its maximum after 40 minutes and then stabilizing, indicating that equilibrium had been achieved. Increasing the methanol-to-oil ratio from 1:3 to 1:6 further enhanced conversion, consistent with Le Chatelier's principle, where higher reactant concentrations drive the reaction towards ester formation.

The MCM-41 catalyst plays a crucial role in enhancing the esterification reaction due to its mesoporous structure and high surface area, which provides a greater number of active sites for the reaction. The uniform pore structure facilitates improved interaction between the reactants and catalyst, enhancing the diffusion of reactants and products, and ultimately increasing the reaction efficiency and conversion rate without the need for excessive catalyst amounts.

#### **3.4.6. Effect of Catalyst Amount ( $A$ ) and Reaction Time ( $D$ )**

The effect of MCM-41 catalyst amount ( $A$ ) and reaction time ( $D$ ) on free fatty acid conversion to esters was studied at 60°C with a molar ratio ( $M$ ) of 1:6. Using 0.1 g of MCM-41 showed superior conversion efficiency, particularly during the first 30 minutes, compared to 0.05 g. This is attributed to the higher availability of active sites in 0.1 g, enhancing catalytic performance. After 40 minutes, conversion rates plateaued for both amounts, suggesting 0.1 g is opti-

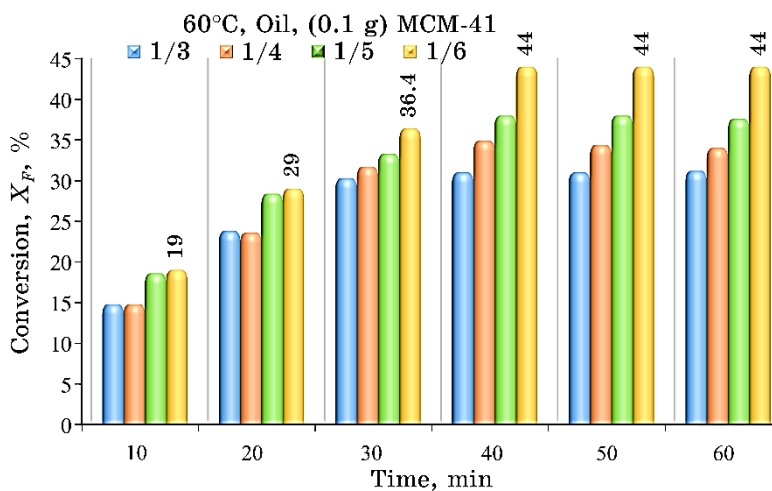


**Fig. 8.** Effect of the methanol-to-oil ratio ( $M$ ) and reaction time ( $D$ ) on the conversion of the refined blend (0.1 g of catalyst).

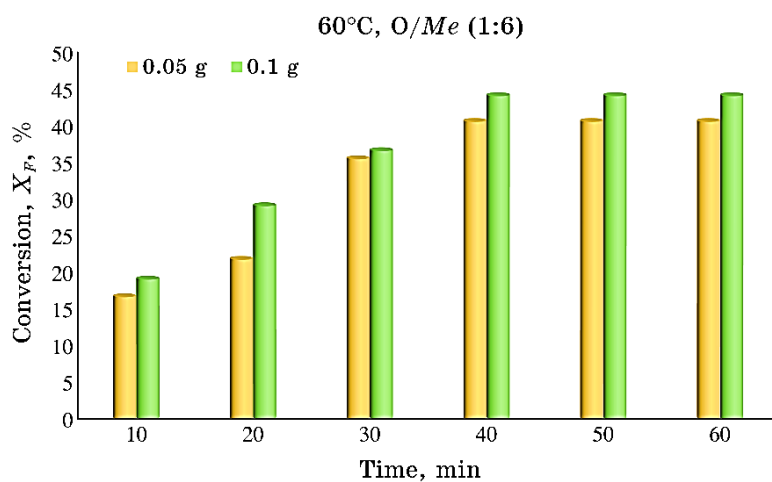


**Fig. 9.** Effect of catalyst amount ( $A$ ) and reaction time ( $D$ ) on the conversion of the refined blend.

mal for efficient esterification within a shorter reaction time, as shown in Fig. 9.

#### 4. CONCLUSIONS

This study successfully prepared and characterized MCM-41, a mesoporous silica-based nanoparticle catalyst, achieving nanoscale di-

mensions 30–50 nm with a highly uniform structure. The catalyst superior properties, such as a large surface area and high thermal stability, significantly enhanced the esterification of free fatty acids in a refined blend of palm and cottonseed oils. Optimal biodiesel production was achieved under the following conditions: a methanol-to-oil molar ratio of 1:6, a catalyst amount of 0.1 g, a reaction temperature of 60°C, and a reaction time of 40 minutes. These findings highlight the potential of MCM-41 as a cost-effective and efficient catalyst for biodiesel production, contributing to the development of sustainable energy solutions.

## 5. HIGHLIGHTS

Successfully prepared MCM-41 with nanoscale dimensions (30–50 nm), confirmed by SEM and XRD analysis.

MCM-41 demonstrated superior catalytic performance, achieving high conversion rates in biodiesel production.

Identified optimal methanol-to-oil ratio (1:6), catalyst amount (0.1 g), and reaction time (40 minutes).

Highlighted MCM-41 potential for efficient, eco-friendly biodiesel production from refined oil blends.

Improved biodiesel properties by blending palm and cottonseed oils, enhancing both low-temperature flow and oxidative stability.

## REFERENCES

1. Mingxin Guo, Weiping Song, and Jeremy Buhain, *Renewable and Sustainable Energy Reviews*, **42**, Iss. 20: 712 (2015); <https://doi.org/10.1016/j.rser.2014.10.013>
2. Donato A. G. Aranda, Rafael T. P. Santos, Neyda C. O. Tapanes, Andr  Luis Dantas Ramos and Octavio Augusto C. Antunes, *Catal. Lett.*, **122**, Iss. 1–2: 20 (2008); <https://doi.org/10.1007/s10562-007-9318-z>
3. Luqman Razzaq, Shahid Imran, Zahid Anwar, Muhammad Farooq, Muhammad Mujtaba Abbas, Haris Mehmood Khan, Tahir Asif, Muhammad Amjad, Manzoore Elahi M. Soudagar, Nabeel Shaukat, I. M. Rizwanul Fattah, and S. M. Ashrafur Rahman, *Energies*, **13**, Iss. 22: 5941 (2020); <https://doi.org/10.3390/en13225941>
4. G. Mutezo and J. Mulopo, *Renewable and Sustainable Energy Reviews*, **137**, Iss. 1: 1106091 (2021); <https://doi.org/10.1016/j.rser.2020.110609>
5. M. E. Borges and L. Diaz, *Renewable and Sustainable Energy Reviews*, **16**, Iss. 5: 2839 (2012); <https://doi.org/10.1016/j.rser.2012.01.071>
6. Qian Zeng, Zhen Song, Hao Qin, Hongye Cheng, Lifang Chen, Ming Pan, Yi Heng, and Zhiwen Qi, *Catal. Today*, **339**: 113 (2020); <https://doi.org/10.1016/j.cattod.2019.03.052>
7. Shweta J. Malode, K. Keerthi Prabhu, Ronald J. Mascarenhas, Nagaraj P. Shetti, and Tejraj M. Aminabhavi, *Energy Conversion and Management*:

- X, **10**, Iss. 1: 100070 (2021); <https://doi.org/10.1016/j.ecmx.2020.100070>
8. Umer Rashid, Muhammad Ibrahim, Shahid Yasin, Robiah Yunus, Y. H. Taufiq-Yap, and Gerhard Knothe, *Ind. Crops Prod.*, **45**, Iss. 1: 355 (2013); <https://doi.org/10.1016/j.inderop.2012.12.039>
  9. Kahraman Bozbas, *Renewable and Sustainable Energy Reviews*, **12**, Iss. 2: 542 (2008); <https://doi.org/10.1016/j.rser.2005.06.001>
  10. Matt Johnston and Tracey Holloway, *Environmental Science & Technology*, **41**, Iss. 23: 7967 (2007); <https://doi.org/10.1021/es062459k>
  11. Venkatesh Mandari and Santhosh Kumar Devarai, *BioEnergy Res.*, **15**, Iss. 2: 935 (2022); <https://doi.org/10.1007/s12155-021-10333-w>
  12. Mohd Aznan Abdul Latif, Ahmad Anas Yusof, Ahmad Zaki Shukor, Farah Aqilah Habidi, Nur Fathiah Mohd Nor, Mohd Zaid Akop, Mohd Hafidzal mohd Hanafi, and Aiman Roslizar, *MATEC Web Conf.*, **90**: 01046 (2017); <https://doi.org/10.1051/mateconf/20179001046>
  13. Anton A. Kiss, Alexandre C. Dimian, and Gadi Rothenberg, *Energy Fuels*, **22**, Iss. 1: 598 (2008); <https://doi.org/10.1021/ef700265y>
  14. Ayhan Demirbas, *Energy Convers. Manag.*, **50**, Iss. 1: 14 (2009); <https://doi.org/10.1016/j.enconman.2008.09.001>
  15. S. N. Yusof, S. M. Basharie, N. A. Sidik, Y. Asako, and S. B. Mohamed, *J. Adv. Res. Fluid Mech. Therm. Sci.*, **86**, Iss. 2: 136 (2021); <https://doi.org/10.37934/arfmts.86.2.136146>
  16. Ahmad Abbaszaadeh, Barat Ghobadian, Mohammad Reza Omidkhah, and Gholamhassan Najafi, *Energy Convers. Manag.*, **63**: 138 (2012); <https://doi.org/10.1016/j.enconman.2012.02.027>
  17. Lay L. Myint and Mahmoud M. El-Halwagi, *Clean Technol. Environ. Policy*, **11**, Iss. 1: 263 (2009); <https://doi.org/10.1007/s10098-008-0156-5>
  18. Ahmad Hafiidz Mohammad Fauzi, Nor Aishah Saidina Amin, and Ramli Mat, *Appl. Energy*, **114**: 809 (2014); <https://doi.org/10.1016/j.apenergy.2013.10.011>
  19. V. N. Ariharan, V. N. Meena Devi, and P. Nagendra Prasad, *Res. J. Pharm. Biol. Chem. Sci.*, **4**, Iss. 2: 1336 (2013); [https://www.rjpbcs.com/pdf/2013\\_4\(2\)/\[145\].pdf](https://www.rjpbcs.com/pdf/2013_4(2)/[145].pdf)
  20. N. Saifuddin, K. Aisswarya, Y. P. Juan, and P. Priatharsini, *J. Appl. Sci.*, **15**, Iss. 8: 1045 (2015); <https://doi.org/10.3923/jas.2015.1045.1058>
  21. Ming Chai, Qingshi Tu, Mingming Lu, and Y. Jeffrey Yang, *Fuel Process. Technol.*, **125**, Iss. 1: 106 (2014); <https://doi.org/10.1016/j.fuproc.2014.03.025>
  22. T. Srinivasa Reddy and M. C. Santhosh Kumar, *Ceram. Int.*, **42**, Iss. 10: 12262 (2016); <https://doi.org/10.1016/j.ceramint.2016.04.172>